Lags in the response of plant assemblages to global warming depends on temperature-change velocity

Authors

L. Camila Pacheco-Riaño[1*]

ORCID iD: https://orcid.org/0000-0002-8539-4816

Fride Høistad Schei [2]

ORCID iD: https://orcid.org/0000-0001-8083-4045

Suzette G. A. Flantua[3±]

ORCID iD: https://orcid.org/0000-0001-6526-3037

John-Arvid Grytnes1[±]

ORCID iD: https://orcid.org/0000-0002-6365-9676

Affiliations

[1]Department of Biological Sciences, University of Bergen, PO Box 7803, 5020, Bergen, Norway.

[2] Norwegian Institute of Bioeconomy Research, Thormøhlensgate 55, 5006 Bergen, Norway.

[3] Department of Biological Sciences, University of Bergen, and Bjerknes Centre for Climate Research, N-5020 Bergen, Norway

* Corresponding author: pachecoriano.c@gmail.com

[±] Joint senior authors.

Acknowledgements:

We thank Tuija Maliniemi, Jonathan Lenoir, and Romain Bertrand for their helpful comments on previous manuscript versions. We would also like to thank Arnaud Gallou for his technical support in R and Cathy Jenks for proofreading the manuscript. SGAF was supported by the European Research Council under the EU Horizon 2020 research and Innovation Programme (grant 741413, Humans on Planet Earth–Long-term impacts on biosphere dynamics), by the TMS-Starting Grant Program funded by Trond Mohn Stiftelse (TMS) and University of Bergen (TMS2022STG03). LCPR was supported by Olaf Grolle Olsen's Scholarship (grant 20019/53/FOL).

Conflict of Interest Statement: The authors have no conflict of interest to declare

Author contributions:

LCPR and JAG designed the study, methodology and modelling approach. LCPR performed all the analyses and led the writing. SGAF and JAG supervised the project. All authors contributed actively to the writing to improve clarity and discussed and commented on the results.

Running title:
Plant lags are linked to temperature-change velocity

Abstract

Aim: Current global warming is driving changes in biological assemblages by increasing the number of thermophilic species while reducing the number of cold-adapted species, leading to thermophilization of these assemblages. However, there is increasing evidence that thermophilization might not keep pace with global warming, resulting in thermal lags. Here, we quantify the magnitude of thermal lags of plant assemblages in Norway during the last century and assess how their spatio-temporal variation is related to variables associated with temperature-change velocity, topographic heterogeneity, and habitat type.

Location: Norway

Time period: 1905 - 2007

Major taxa studied: Vascular plants

Methods: We inferred floristic temperature from 16,351 plant assemblages and calculated floristic temperature anomaly (difference between floristic temperature and baseline temperature) and thermal lag index (difference between reconstructed floristic temperature and observed climatic temperature) from 1905 until 2007. Using generalized least square models, we analyzed how the variation in observed lags since 1980 is related to temperature-change velocity (measured as magnitude, rate of temperature change, and distance to past analogous thermal conditions), topographic heterogeneity, and habitat type (forest vs non-forest).

Results: The floristic temperature anomaly increases overall during the study period. However, thermophilization falls behind temperature change, causing a constantly increasing lag for the same period. The thermal lag index increases most strongly in the

period after 1980, when it is best explained by variables related to temperature-change velocity. We also find a higher lag in non-forested areas, while no relationship is detected between the degree of thermal lag and fine-scale topographic heterogeneity.

Main conclusions: The thermal lag of plant assemblages has increased as global warming outpaces thermophilization responses. The current lag is associated with different dimensions of temperature-change velocity at a broad landscape scale, suggesting specifically that limited migration is an important contributor to the observed lags.

Keywords

lag dynamics, mountain biodiversity, plant assemblages, shifting isotherms, migration lag, thermophilization

1 | INTRODUCTION

Current global warming is causing a global redistribution of species at different spatial scales with general poleward and upward shifts (Chen, Hill, Ohlemüller, Roy, & Thomas, 2011; Feeley, Bravo-Avila, Fadrique, Perez, & Zuleta, 2020; Lenoir et al., 2020; Lenoir & Svenning, 2015; Rumpf et al., 2019; Steinbauer et al., 2018). Such directional shifts in species ranges cause changes in local plant assemblages, with thermophilic species increasing and cold-adapted species decreasing, resulting in a thermophilization of the assemblages (Blonder et al., 2015; De Frenne et al., 2013; Gottfried et al., 2012). A growing number of studies suggest that the thermophilization of plant assemblages fails to keep pace with global warming (Bertrand et al., 2011; Freeman, Song, Feeley, & Zhu, 2021; Lenoir et al., 2020; Richard et al., 2021). Such delayed responses result in a so-called ´climatic lag´ or ´climate debt´, i.e. a discrepancy between the thermophilization response of the species assemblages and observed changes in climate. Given that these responses are related explicitly to temperature, we use the terms ´thermal lag´ and ´thermal debt´ to differentiate from studies that also include other climate variables alongside temperature.

Thermal lags have been detected across a broad range of taxa and ecosystems, but with considerable variation in magnitude (Lenoir et al., 2020). For example, lowland forest assemblages in France are found to lag further behind shifting isotherms at the macroclimate scale than highland forest assemblages (Bertrand et al., 2011). Likewise, temperate

mountain assemblages are shown to be slower at tracking macroclimate temperature change than assemblages on tropical mountains (Freeman et al., 2021).

Quantifying the magnitude of thermal lags and assessing the main underlying determinants for variations in thermal lags is needed to enhance our knowledge of broad-scale assemblage dynamics. Bertrand and collaborators (2016) observed that greater thermal lag occurs in plant assemblages found in historically warmer areas, and a recent study by Richard et al. (2021) found that forest-structure traits (e.g. stand age) and natural and anthropogenic disturbances modulate thermal lags in understory forest assemblages by altering microclimate conditions. However, we still need a better understanding of the spatio-temporal patterns of thermal lags to assess the impact of global warming on biodiversity and ecosystem functioning (Bertrand, 2019; Blonder et al., 2015; Svenning & Sandel, 2013).

Another important factor to consider when trying to understand the causes of thermal lags is temperature-change velocity, i.e. the spatial distance a species must migrate per time unit to keep track of changing temperatures. This velocity is related to both the degree of temperature change and to how steep the temperature gradient is across spatial gradients (Garcia, Cabeza, Rahbek, & Araújo, 2014; Loarie et al., 2009). Areas with high topographic heterogeneity at broad scales will generally have lower temperature-change velocity as steep elevational gradients cover a wide temperature range within short geographical distances (Loarie et al., 2009). As a result, plant species may only need to shift short distances to find thermally suitable habitats in areas with low temperature-change velocity when climate is changing. On the other hand, if species migration is limited by dispersion and high temperature velocities occur, a greater thermal lag is more likely (Bertrand, 2019; Bertrand et al., 2016; Jump, Mátyás, & Peñuelas, 2009; Lenoir et al., 2020). Therefore, we expect the magnitude of thermal lag to be positively related to both temperature change (magnitude and rate of change) and the spatial distance plant species need to migrate to find analogous thermal conditions (i.e. conditions in which they occurred before the onset of global warming).

Using a macroclimatic approach may overlook microclimatic variation that allows species to survive in a microclimatically heterogenous landscape (De Frenne et al., 2013; Graae et al., 2018; Richard et al., 2021). Assuming that local species extirpations and colonization reflect an equilibrium condition between local thermophilization and microclimate, topographic heterogeneity at finer landscape scales may result in a perceived disequilibrium between thermophilization and macroclimatic conditions. Using broad-scale estimates of thermal

conditions may therefore lead to a greater perceived thermal lag in areas of fine-scale topographical heterogeneity (Alexander et al., 2018; De Frenne et al., 2013).

In addition to topographic heterogeneity, the forest canopy may also affect macrothermal lags through microclimatic conditions. Some studies have demonstrated that thermal lag in forest plant assemblages is lower, as macroclimatic warming is buffered by canopy cover modifying the microclimate (De Frenne et al., 2019; Richard et al., 2021; Zellweger et al., 2020). Hence, the forest structure provides thermal microrefugia for species persistence (Zellweger et al., 2020). Based on these findings, we also expect to find a larger macrothermal lag in forested areas than in non-forested areas.

Our main aim is to quantify the magnitude of thermal lags of plant assemblages in Norway during the last century and assess how their spatio-temporal variation is related to variables associated with (i) temperature-change velocity, (ii) topographic heterogeneity at fine landscape scales, and (iii) habitat type (forest vs. non forest). To address this aim, we established a relationship between plant assemblages and temperature during a baseline period (before recent global warming), and subsequently inferred a floristic temperature from the composition of these assemblages. We use floristic temperature anomaly as our proxy for thermophilization which is represented by the difference between the floristic temperature and the temperature of the baseline period. The thermal lag index was correspondingly determined by taking the difference between the floristic temperature and the observed temperature of the sample year.

We assessed the temporal trend of the floristic temperature anomaly and the thermal lag over the course of the 20th century. We then focused on the thermal lag after the onset of climate warming in the region and investigated how baseline temperature, temperature-change velocity, topographic heterogeneity, and habitat type (forest vs non-forest) are related to the thermal lag magnitude.

We expect to find the most pronounced lag in warmer baseline conditions with the highest temperature-change velocities, i.e. higher rates of temperature change and/or longer distances to past analogous temperatures (Alexander et al., 2018; Loarie et al., 2009). On a fine landscape scale, we expect to find more pronounced macrothermal lags in landscapes with high topographic heterogeneity (due to a higher probability of finding suitable microclimatic conditions and microthermal refugium within a short distance). In contrast, we

expect smaller lags in forested areas caused by the buffering effect of the canopy cover (Bertrand et al., 2016; Zellweger et al., 2020).

2 | MATERIALS AND METHODS

We illustrate the workflow of our analyses in Figure 1 from the data compilation step (climate and plant assemblages) to the identification of the temperature breaking point and the subsets used for the analyses (Historical, Baseline, Contemporary), followed by the estimation of the floristic temperature anomaly and thermal lag index, and the final analysis related to the temporal trends and possible determinants of temporal lag.

Compilation of plant assemblages (Figure 1a)

We compiled an occurrence dataset from the Global Biodiversity Information Facility (GBIF), containing 605,637 records of terrestrial vascular plant species distributed across Norway. These datasets are species check-lists from individual locations that have been curated, digitized, and deposited to GBIF as occurrence data by university museums (Norwegian University of Life Sciences, 2019; Norwegian University of Science and Technology, 2021; University of Agder, 2021; University of Oslo, 2019a, 2019b). Each species occurrence in this dataset is provided with information on geographical coordinates, survey date, and collector(s). We standardized the coordinates for consistency and deleted occurrences with obviously incorrect coordinates, e.g. keeping only records within the Norwegian mainland. We harmonized the taxonomy using GBIF's backbone taxonomy (The Global Biodiversity Information Facility, 2020). After these steps, we checked the species lists and merged sub-species to the species level, removing non-vascular species and taxa identified at the genus level or above. We also deleted duplicated records that came with the same species names, coordinates, years, and collector(s) (e.g. as a result of merging subspecies). Only some of the species' occurrences had elevation information, often as a minimum and maximum elevation (meters above sea level – m a.s.l.). Therefore, we extracted elevation values for all sampling points from a digital elevation model (DEM) at 25 m resolution obtained from the Copernicus Program (Copernicus, 2016). This process resulted in a cleaned dataset compilation of 511,170 occurrence records of plant species observations spread out over Norway.

We reconstructed assemblages by assuming that a unique coordinate, survey date, and collector represented a unique species assemblage and grouped the occurrence data by

coordinates, date, and collector. After reconstructing the assemblages, we only kept species that occurred in more than five assemblages and only retained assemblages containing a minimum of five species. With these criteria, we ensured having sufficient species representation in each assemblage to estimate floristic temperature using a ´transfer function´ (see the section on Thermal lag index) (Bhatta, Grytnes, & Vetaas, 2018). This resulted in a dataset compilation of 17,086 plant assemblages covering 1,111 species (**see Supplementary Information Table S1 for the full species list**). The assemblages were sampled from the beginning of the 20th century until 2007. The sampling sizes of these assemblages are unknown and probably vary from a few square meters to more than one square kilometer. This is also reflected in the number of species per assemblage which ranges from 5 to 295, with an average of 10 species (SD ±11, see also **Supplementary Information Figure S1**), indicating that most assemblages represent a relatively small area. There were 76 assemblages with more than 80 species, and six of them are in the contemporary dataset. The crucial assumption for the analyses we have done is that the occurrences within a single assemblage represent the same macroclimatic conditions. Based on our knowledge of the original check-lists, we anticipate this to be a reasonable assumption and, given the large variation in macroclimatic variation between assemblages in this dataset, we can assume that any deviation within assemblages will be minor compared to the main trends between assemblages.

Temperature data, break-point analysis, and dataset subsets

We obtained macroclimatic temperature data (**Figure 1b**) from the global climate dataset CHELSAcruts at 30 arc-seconds (~1 km) resolution (Karger et al., 2017; Karger & Zimmermann, 2018), covering the time period from 1900 to 2016. For each assemblage, we calculated the following climatic variables: i) mean annual temperature (MAT), ii) mean temperature of the coldest month (Tcm), and iii) mean temperature of the warmest month (Twm). Each temperature variable was calculated based on an average of five years prior to the vegetation sampling year (including the survey year) to smooth out atypical extreme fluctuations (following Steinbauer et al., 2018).

The analyses of floristic temperature anomaly and thermal lag only allow one temperature variable to be used. To select the temperature variable among the three potential variables (MAT, Tcm, Twm) that best explains the variation in species composition we used nonmetric multidimensional scaling (NMDS) ordination on the species assemblage dataset on a subset of the data from the time period prior to major temperature changes (Baseline subset; see

below) and added the three temperature variables passively. These preliminary analyses showed that mean annual temperature had the strongest correlation with plant assemblages (R^2 =0.56), followed by Twm (R^2 =0.42) and Tcm (R^2 =0.37) (**Figure S2**). Therefore, we used mean annual temperature for all remaining analyses. The ordination analysis was conducted using the R package *vegan*, version 2.5-7 (Oksanen et al., 2013).

To identify a time period of relatively stable temperature, we used a break-point analysis to identify the specific year that the trend of temperature increase started within our study area (**Figure 1c**). We performed a structural change analysis to find break-points using a Bayesian information criterion (BIC) (Andrews, 1993) and the *strucchange* package (Zeileis, Leisch, Homik, & Kleiber, 2002). The break-point analysis for the full period suggested only one break-point in mean annual temperature in the year 1988 (95% CI from 1983 to 1995, **Figure 2a, Figure S3**). Based on this, we selected a period in advance of this break-point to establish a relationship between species assemblages and temperature. To make sure that the temperature increase did not influence our relationship we selected 1979 as the end year of this period and found that starting in 1950 ensured a large enough dataset to train the model. As a result we divided the species assemblage data into three subsets (**Figure 1d, Figure S4**): 1) Historical subset: for use in the backward prediction and also to evaluate the robustness of the model (years 1905 to 1949; 6,279 assemblages), 2) Baseline subset: the period before the temperature break-point with the purpose to train the transfer function (years 1950 to 1979; 4,109 assemblages), and 3) Contemporary subset: for use in the forward prediction and the thermal lag drivers analysis (years 1980 to 2007; 6,698 assemblages).

Floristic temperature anomaly and thermal lag index

We inferred the floristic temperature **(Figure 1e**) using a ´transfer function´ based on the Hutchinsonian niche concept (Hutchinson, 1957), which assumes a unimodal response curve with an ecological optimum of species with respect to the climate variable considered. Hence, species assemblages can be used to infer climatic conditions of a particular area and time period (Birks & Simpson, 2013). This modeling approach has been one of the most widely used methods to reconstruct terrestrial paleoclimates (Chevalier et al., 2020). In paleoclimatology, a transfer function is established by finding the relationship between species assemblages and a specific climate variable for a training dataset from present-day assemblages (Salonen et al., 2011). This function is then used to reconstruct past climates from fossil assemblage data (Salonen et al., 2011). This principle can be applied more

broadly to climatic variables, which can be inferred from the assemblage in the training set during a specific time period. This can then be used to infer climatic conditions from assemblages during other periods of time (Bertrand et al., 2011; Riofrío-Dillon, Bertrand, & Gégout, 2012).

We built our transfer function by first establishing the relationship between species in the assemblages and temperature using the Baseline period (1950–1979) as the training dataset, and then inferring the floristic temperature from the assemblages during the Historical (1905–1949) and Contemporary periods (1980–2007). To minimize geographical bias when making the transfer function, we only used assemblages that were at least 500 m apart. We also used NMDS to detect and remove any unusual assemblages (we identified and removed two outlying assemblages) before using the Baseline subset to create the transfer function. To estimate the floristic temperature, we used weighted averaging partial least squares (WA-PLS) (ter Braak & Juggins, 1993), which is a powerful inverse approach widely used to reconstruct climates in paleoecology (Liu, Prentice, ter Braak, & Harrison, 2020; ter Braak & Juggins, 1993). The performance of the transfer function models was assessed by leave-one-out cross-validation. We selected the most significant component with the lowest root mean square error of prediction (RMSEP), the highest R^2, and the lowest maximum bias (Liu et al., 2020). We also evaluated weighted averaging (WA) with different deshrinking (classical, inverse, or monotonic) techniques following Bhatta, Birks, Grytnes, & Vetaas (2019) but these did not improve the model. The transfer function analysis was performed using the *fxTWAPLS* package (Liu et al., 2020).

One issue with WA-PLS is that estimated values based on the training dataset tend to be higher than observed values at the low end of the temperature range, and lower at the high end (Liu et al., 2020). To address this bias, we removed assemblages with extreme temperatures in the prediction phase and only included assemblages in the climatic temperature range between -2.5 and 8.5°C (**Figure S5**). As a result, the final dataset consists of 16,351 assemblages (Historical subset: 6,094 assemblages, Baseline subset: 4,049 assemblages, and Contemporary subset: 6,208 assemblages). Since the overestimation at both ends persisted in the residuals, we subsequently used the residuals of the WA-PLS model to fit a local nonparametric regression (LOESS) with a span of 0.75 to correct for the remaining bias in the used temperature range. Finally, we corrected the predictions of the WA-PLS using the difference between the residuals from the WA-PLS and LOESS models

to infer the floristic temperature (**Figure S5**). This procedure was then used to estimate the floristic temperature for each assemblage in the full dataset.

As a proxy of thermophilization we calculated the floristic temperature anomaly as the difference between the floristic temperature and baseline temperature within a 1 km^2 grid cell (mean $MAT_{1950\text{-}1979}$) for each assemblage (**Figure 1f**). A positive value indicates an increase in the floristic temperature (meaning increasing number of thermophilic species and/or a decrease of cold-adapted species) compared to the baseline period (1950-1979).

To estimate the presence and magnitude of thermal lags, we calculated a thermal lag index for each assemblage represented by the difference between the estimated floristic temperature and the observed macroclimatic temperature for the sample year (i.e. the average for the five years prior to sampling) (**Figure 1f**). The thermal lag index will be zero when the relationship between plant assemblages and climate during the Contemporary period (1980–2007) is the same as during the Baseline period (1950–1979). A positive thermal lag index would be found when the floristically inferred temperature is lower than the observed temperature, and indicates that plant assemblages lag behind the estimated warming (Bertrand et al., 2011). Note that with this approach the observed temperature difference between the baseline temperature and the observed temperature at the year of sampling is equal to the sum of the floristic temperature anomaly and thermal lag.. This means that the variation we observe in thermal lag will be 100% explained by a model containing the floristic temperature anomaly and the observed temperature change. Additionally, the transfer function, predictions, and comparison with observed temperatures are all based on macroclimatic data with a resolution of 1 km, meaning that the thermal lag index is a macrothermal lag. A microthermal equilibrium might still be a possibility with a large microclimatic heterogeneity within the 1 km cells, even if a large macrothermal lag is observed.

Temporal analysis of floristic temperature anomaly and thermal lag

Prior to the analyses of what causes the magnitude of lags in the Contemporary period, we assessed the temporal trends of floristic temperature anomaly and thermal lag indices during the full study period (1905–2007; **Figure 1g**). Because different geographic areas have warmed differently within Norway, the overall temperature trend is not directly comparable with the average floristic temperature anomaly (or thermal lag) trends using all samples. To be able to compare these trends with the overall temperature trend for Norway, we therefore

first removed potential spatio-temporal bias in the distribution of the assemblages. To do so, we divided Norway into seven geographical zones (**Figure S7**) and five-year time intervals and performed a stratified random sampling of five assemblages from each zone and time interval. Next, we assessed the temporal variation of the floristic temperature anomaly and the thermal lag using a generalized least square (GLS) model using the spatio-temporal bias-corrected dataset. To explore any non-linear trends, we also visualized any trends by fitting generalized additive models (GAMs) with a logit link and smooth functions of k=4. After comparing the temporal trend of the thermal lag based on the uncorrected vs. bias-corrected dataset (see **Figure S8** a vs. b, respectively) we performed all analyses showing the temporal trends with the latter dataset.

Determinants of thermal lag in the contemporary period

By using the Contemporary subset, we assessed the relationship between the thermal lag index of each assemblage and (a) baseline temperature conditions, (b) temperature-change velocity, (c) topographic heterogeneity at fine landscape scales, and (d) habitat type (forest cs non-forest cover) **(Figure 1h**).

Macroscale

(a) Baseline temperature conditions: Previous research has shown baseline MAT to be an important determinant of thermal lags in plant assemblages (Bertrand et al., 2016). Therefore, we computed baseline temperature conditions from CHELSA as the average of $MAT_{1950\text{-}1979}$ values, i.e. 30-year average normally used to capture long-term climatic conditions.

(b) Temperature-change velocity: To represent the velocity of temperature change, we calculated three different variables, namely (i) distance to past analogous thermal conditions, (ii) magnitude of temperature change, and (iii) rate of temperature change. Distance to past analogous thermal conditions was calculated by first identifying the temperature of the point of the assemblage at the time of sampling (as a five-year average before sampling) and then quantified the minimum Euclidean geographic distance to a location with the same temperature during the period of 1969–1979. The calculated distance represents the distance species have to migrate to encounter the same temperature as they had before global warming and is influenced by the magnitude of temperature change and broad-scale topographic heterogeneity. Distances were calculated using the R-package *nngeo* (Dorman, Rush, Hough, Russel, & Karney, 2020). The

magnitude of temperature change was estimated as the temperature change over time since the baseline period (i.e. since 1979). We estimated the rate of temperature change as:

$$Rate\ of\ temperature\ change = \frac{Temp\ (survey\ year) - Temp\ (reference\ year)}{survey\ year - reference\ year}$$

where *Temp (reference year)* is the average temperature during the Baseline period (1950–1979) at each assemblage location, and *reference year* is set to 1979. *Temp (survey year)* is the 5-year average prior to the survey year for each assemblage location, and *survey year* is the year of sampling for each assemblage. The outcomes represent thermal rate of change since 1979.

Fine-scale

(c) Topographic heterogeneity at fine landscape scales: Here we calculated the following topographic variables: (i) mean elevation, (ii) terrain ruggedness index (ruggedness), and (iii) Shannon index of geomorphological landforms. We derived these variables from the 25-m resolution DEM obtained from the Copernicus Program (Copernicus, 2016). Although mean elevation is not a direct measure of topographic heterogeneity, we included this variable as heterogeneity tends to increase with increasing elevation (**Figure S10**). We calculated the latter two variables by applying the methodology proposed by Amatulli et al. (2018). Terrain ruggedness measures the spatial variability in elevation and is estimated by the mean of the absolute differences in elevation between a center cell and its eight surrounding cells, i.e. this is a measure of heterogeneity within 3 x 3 grid cells (75 x 75 m) around the location of the sampled assemblage (Riley, DeGloria, & Elliot, 1999). Here, flat areas have a value of zero, whereas topographic heterogeneous areas have positive values (Amatulli et al., 2018). The Shannon index of geomorphological landforms categorizes the spatial variability within a certain area with the relative proportion of grid cells covered by landform types within a 3 x 3 window (75 x 75 m). Landform types include flat, peak, ridge, shoulder, spur, slope, hollow, foot slope, valley, and pit (Amatulli et al., 2018). For this study and following Amatulli et al. (2018), the Shannon index represents the diversity of the land types in a 10 x 10 window (250 meters); higher values indicate a higher diversity of landforms (Amatulli et al., 2018).

(d) Habitat type (Forest vs-non Forest cover) : By using the Corine Landcover (CLC) for Norway (NIBIO, 2021), we determined for each assemblage whether its location concurred with the vegetation type classified as forest. We included the following CLC as forest cover:

"Forest" and "Shrub and /or herbaceous vegetation". We assessed if setting the limit at different forest types (as defined by CLC) had an impact on the GLS models but found that this is not the case. Therefore, we include all the landcover types already mentioned as forest.

To define the relationship between the thermal lag index and the above-mentioned variables, we used GLS models. Using the assemblages' locations, we fitted different spatial correlation structures to account for spatial autocorrelation. The exponential spatial correlation with a nugget effect was selected based on its performance given by the Akaike information criterion (AIC) and spatial autocorrelation in residuals. Even after this step, a low degree of spatial autocorrelation remained in the residuals (**Figure S11**). We test-ran a limited number of models without any spatial autocorrelation but demands on computer resources multiplied manifold without substantial change in the outcomes. In addition, small levels of autocorrelation in the residuals do not necessarily indicate a critical issue in the model fitting (Beale, Lennon, Yearsley, Brewer, & Elston, 2010). We, therefore, opted to accept the low degree of spatial autocorrelation as depicted in **Figure S11**.

We used the Contemporary dataset (1980–2007) to assess each explanatory variable separately **(Figure 1h**). When evaluating the univariate models, we included the year of the assemblage sampling as a covariable to account for the temporal variation in the thermal lag prior to testing of each variable. We subsequently built three multivariate models. The first one focuses on the macroscale baseline temperature and temperature-change velocity (i.e. rate of temperature change and distance to past analogous thermal conditions). The second one includes the above variables plus the magnitude of temperature change. In this model, we excluded year as an explanatory variable due to its high correlation with the magnitude of temperature change (Spearman's r coefficient > 0.6, **Figure S12**). The third model focuses on the fine-scale topographic heterogeneity (i.e. mean elevation, ruggedness, Shannon index of landforms) and forest cover. Finally, we built a full model including all variables, but since rate of temperature change and magnitude of temperature change were highly correlated, we built two different models each including all the explanatory variables but one of either of the temperature-change variables. We assessed the goodness-of-fit for each GLS model through AIC where we gave preference to models with the lowest values of AIC. As a measure of goodness-of-fit, we computed the R^2 likelihood-ratio using the *rr2* package (Ives & Li, 2018). Note that correlation values among all our explanatory variables included in each of the full models did not exceed a Spearman's r coefficient of 0.6 **(Figure S12**).

We conducted all data handling and analyses, and the creation of figures in the programming environment ***R*** v.4.2.0 (R Core Team, 2021). All GLS models were developed using the *nlme* package (Pinheiro, Bates, DebRoy, & Sarkar, 2020). Other R-packages used for data handling and extraction and graphical visualization are: *tidyverse v.1.3.1* (Wickham et al., 2019) , *raster 3.5-15* (Hijmans, Robert J. ; van Etten, 2012), *sf v.1.0-9* (Pebesma, 2018), and *ggpubr v.0.4.0* (Kassambara, 2020).

3 | RESULTS

Temporal trends of observed temperature and break-point (Figure 1c)

We find a constant increase in temperature since the beginning of the century (1905–2007, 9.8×10^{-3}°C yr^{-1}, 95% confidence interval (CI): 0.005–0.014), with an endpoint of 1.77°C for 2007 compared to the overall mean of the baseline period (**Figure 2a)**. The break-point analysis suggests one break-point in 1988. The temperature was relatively stable from 1900 until 1988 (-7.2×10^{-5}°C yr^{-1}, 95% CI: -0.008–0.005). From 1988, we find a temperature break-point followed by a steep increase in temperature afterward (linear regressions indicate that average temperatures in Norway increased by ~ 2.24×10^{-2}°C yr^{-1}, (CI: -0.02-0.07) **Figure 2a**. The decade before 1988 was relatively cold, with the coldest five-year average occurring during 1980.

Transfer function and floristic temperature reconstruction (Figure 1e-f)

The transfer WA-PLS regression was built using the Baseline subset (1950–1979) which included 4,109 plant assemblages and 1,111 species. The second component of the WA-PLS model has the smallest RMSEP (1.48), the highest R^2 (0.73), and the lowest maximum bias (8.19). The model performance and comparisons are summarized in **Table S2**, and a scatter plot of the observed temperatures (MAT) against estimated floristic temperatures and their residuals is shown in **Figure S5**. Trimming the temperature edges and the correction fitting of the LOESS significantly improved the relationship between MAT and floristic temperature for the baseline dataset (R^2 reached 0.85). The method used here is built on the assumption that the plant assemblages are in approximate equilibrium during the period used to train the model (i.e. the Baseline period during 1950–1979). To evaluate this assumption, we tested for possible temporal trends in the thermal lag index during the Baseline period, but no statistically significant trend was found (**Figure S13**).

Temporal trends in floristic temperature anomaly and thermal lag index (**Figure 1g**)

A linear regression indicates that the floristic temperature has an increasing trend with time since the beginning of the 20th century, with a slope of 0.003°C yr^{-1} (**Figure 2b**; SE=9 × 10^{-4}, R^2=0.067, p<0.001). Looking at the contemporary period only (1980–2007), this trend is more pronounced with 0.010°C yr^{-1} (SE=0.005, R^2=3.03 × 10^{-3}).

We identified a weak but linear increase in the thermal lag index with time since the beginning of the century (estimated slope = 0.0049 yr^{-1}, R^2=0.079, **Table 1**; **Figure 2c**). During the Contemporary period (1980–2007), the thermal lag index further increased to an average of 0.0493 °C yr^{-1} (SE=0.005, p<0.001; **Table 1**). The GAM regression reveals that both the floristic temperature anomaly and the thermal lag index crudely follow the temperature oscillation during the 20th century (**Figure 2a**). When temperatures were particularly cold (until the end of the 1920s), we find negative floristic temperature anomaly. However, the temperature cooling in this period was still larger than the floristic temperature, and we observe a small negative thermal lag in the same period (**Figure 2c**). Floristic temperature followed temperature increases during the 1930–40s, and for this time period we do not see a thermal lag as the index was close to zero. However, these two events were minor compared with the steadily increasing trend after 1988 (**Figure 2**). According to the additive model, floristic temperature anomaly and thermal lag have increased monotonically since 1988 (**Figure 2 b,c**) with an acceleration towards the beginning of the 21st century. For the endpoint year (2007), the linear models and GAMs suggested a floristic temperature anomaly of 0.37°C and 0.60°C and thermal lag of 0.27°C and 0.51°C, respectively.

Variables influencing floristic temperature anomaly and thermal lag (Figure 1h)

The variations in the floristic temperature anomaly and the thermal lag index during the Contemporary period (1980–2007) are influenced by different variables. On a macroscale, the magnitude of temperature change alone has a strong positive influence on both the floristic temperature anomaly (estimated slope=0.27, R^2=0.085, p=<0.001, **Figure 3a**) and the thermal lag index (estimated slope=0.70, R^2=0.076, **Figure 3d, Table 2**). Hence, assemblages located in areas with high temperature change experienced both higher floristic temperature and larger thermal lags, and our analyses indicate that approximately 30% of the warming is captured by the floristic temperature anomaly, while the remaining 70% remains as thermal lag.

From the univariate models accounting for time, we observe a positive relationship (**Table 2**) between the thermal lag index and distance to past analogous temperatures (estimated slope=0.14, p<0.001 **Figure 3b**, **Table 2**), rate of temperature change (estimated slope=2.13, p<0.001, **Figure 3c, Table 2**), and the baseline temperature (estimated slope=0.02, p<0.001, Figure **3**e, **Table 2**). Hence, larger thermal lags are found in areas i) that are further away from past analogous thermal conditions, ii) that have a higher rate of temperature change, and iii) have warmer baseline conditions. The multivariate model to explain thermal lags for variables related to temperature-change velocity includes time, distance to past analogous thermal conditions, rate of temperature change, and baseline temperature (R^2=0.126, **Table 2**).

At a final scale (**Figure 1h**), topographic heterogeneity explains a lower fraction of the variation in the thermal lag index compared to the temperature-change velocity variables. Including time in the univariate models, we found significant negative relationships between the thermal lag index and terrain ruggedness (estimated slope=- 6.30×10^{-3}, p<0.001, **Figure 3f, Table2**), suggesting that assemblages have a larger thermal lag in less rugged terrains. For both geomorphological landform diversity (**Figure 3g**, **Table 2**) and elevation (**Figure 3h**), the relationship with the thermal lag index is not statistically significant (p>0.05). We detect a significant difference in the lag index between forested and non-forested areas with non-forested areas having on average 0.11 degrees larger lag than forested areas (p <0.001, **Figure 3i**, **Table 2**). The multivariate model combining the variables for topographic heterogeneity and forest cover has an R^2 of 0.042 (**Table 2**) and includes time, elevation, Shannon index for landforms, ruggedness, and forest cover.

The full model including all the variables explains around 14% of the variance. Looking at the marginal contribution (i.e. the contributions after all other variables in the model are included) of the individual explanatory variables reveals that only magnitude of temperature change and distance to past analogous thermal conditions have statistically significant marginal contributions to the variation in the thermal lag index (**Table 3**). None of the variables relating to topographic heterogeneity and forest cover explain a unique proportion of the variance in this model, as indicated by the p-values associated with the marginal contributions (**Table 3**).

4 | DISCUSSION

Our analyses show that temperature in our study area has increased significantly since the onset of the 20th century, and floristic assemblages have experienced clear thermophilization (increase in floristic temperature compared to the baseline period) but also a strong lag in this period. Both the floristic temperature increases and the temperature increase were most pronounced in the period after 1980. However, the observed increase in floristic temperature fails to keep track of the concurrent regional changes in temperature, resulting in a steadily increasing thermal lag of species assemblages since 1980. Our thermal lags are consistent with previous studies around the world for both terrestrial and marine organisms (Lenoir et al., 2020), in different ecoregions across the Americas (Feeley et al., 2020), mountain forests in Taiwan (O'Sullivan, Ruiz-Benito, Chen, & Jump, 2021), and the European Alps (Rumpf et al., 2018).

Our study provides the first evidence on how a thermal lag can change during a longer time period and supports the findings of Lenoir et al. (2013) that high latitudes have an increasing thermal lag over time. Our finding also adds to the mounting evidence that contemporary thermophilization of plant assemblages is occurring across different vegetation types around Europe (Bertrand et al., 2011; Gottfried et al., 2012; Grytnes et al., 2014; Steinbauer et al., 2018). In comparison to other studies, our detected thermophilization (0.010°C yr^{-1}, 1980–2007) is similar to other studies (e.g. 0.02°C in forest lowlands, 1965–2008, Bertrand et al. 2011) or somewhat lower (e.g. 0.08 to 0.10°C in forest, 1995–2015, Richard et al., 2021). Our results indicate that the magnitude of temperature change plays a key role in both thermophilization and thermal lag of plant assemblages, an observation which is in accordance with other studies (De Frenne et al., 2013; Feeley et al., 2020). We also demonstrate that after 1980, the magnitude of thermal lags has a clear spatio-temporal signal related to the temperature-change velocity, as we find that distance to past analogous thermal conditions as well as magnitude and rate of temperature change significantly matter in modulating thermal lags. In agreement with previous studies, our results also show that thermal lag appears to be considerably larger under warmer conditions (e.g. Bertrand et al., 2016; Lenoir et al., 2020; Richard et al., 2021).

Thermal lags can be caused by migration lags or extinction lags. Although it is challenging to disentangle migration and extinction lags for the current analyses, the positive relationship between thermal lags and distance to past analogous thermal conditions found in our study suggests that migration distance plays a role in causing thermal lags. The evidence presented here may therefore suggest that plant assemblages are too dispersal limited to

keep up with the contemporary temperature-change velocities. How migration distance influences thermal lags remains, however, poorly studied under current climate warming. Studies from the European mountains (e.g. Grytnes et al., 2014, Rumpf et al. 2018) failed to find a clear relationship between range shifts and traits associated to species' dispersal capacity (i.e. the degree by which species persist in their range area).

Contrary to our initial expectation, fine-scale topographic heterogeneity and forest cover show a less consistent and generally weaker relationship to our estimates of thermal lags than variables associated with temperature-change velocity. Earlier studies have indicated that microclimatic refugia in topographically heterogeneous terrains can facilitate the persistence of species outside their 'ideal' macroclimatic niche (De Frenne et al., 2019; Graae et al., 2018), resulting in the detection of longer macrothermal lags. Nevertheless, based on the topographic variables used, we find no supporting evidence for an important role for microclimatic refugia in creating macroclimatic thermal lags (**Figure 3 f-h**). This is also the case when considering the buffering effects of forest canopy (Richard et al., 2021; Zellweger et al., 2020), potentially creating a higher perceived thermal lag in forested areas when considering the relationship between species assemblages and macroclimate. When looking at the differences between areas with forest canopy vs non-forested areas, we actually find the opposite pattern with a significantly greater lag in non-forested areas. One possible explanation of this discrepancy may be that a large part of our non-forest areas are from arctic-alpine areas, which generally have a higher number of long-living species compared to forest. Furthermore, the species response in these areas may also be slowed down by other factors, such as soil development or land use (Rumpf et al., 2018). In this context, we also note that we do not find any relationship with elevation, but this may be because the effects of long-lived species and soil development may be counteracted by the effects of distance to past analogous temperatures, which, in general, will be shorter in mountain areas.

It is important to note that our dataset includes a broad spatial and temporal extent, as well as different types of vegetation, resulting in significant variation in the floristic temperature anomalies and thermal lags. This data heterogeneity might be reflected in the low predictive power of the models. However, we argue that regardless of the heterogeneity of the data, empirical studies such as presented here can assess and estimate temperature-change velocity and its ecological importance at the community level.

For many plant species it is unknown how much thermal flexibility remains in their niche space to respond to changing temperatures (Jackson & Sax, 2010), hence it is difficult to know when (or if) the thermal debt will be paid off. Since global warming began several decades ago, we could expect to see some signs of species assemblages catching up with temperature increases, and that thermal lags would stabilize or decrease ('assemblage self-regulation') (Blonder et al., 2015). However, after an initial warming phase and a slow vegetation response at the beginning of the Contemporary period (**Figure 2**), we do not detect any trend suggesting a slowdown or decrease, even after more than 20 years of warming. On the contrary, we detect an accelerating lag towards the present, suggesting that temperature change continues to outpace plant assemblages' responses, as found for understory plants in France (Bertrand et al., 2011; Richard et al., 2021).These findings trigger the question of whether such thermal debts will continue to accumulate, pushing assemblages to potentially critical breakpoints for ecosystem functioning (Alexander et al., 2018; Bertrand et al., 2016; Lenoir et al., 2020), or whether other mechanisms are at play that will prevent loss of species and consequently ecosystems.

Our chosen approach using transfer functions allowed us to gain new insights into the nature and magnitude of vegetation thermal lags in the face of global warming. This approach has previously been tested and used to study the effect of environmental change (Bertrand et al., 2011; Riofrío-Dillon et al., 2012). One of the major assumptions of this approach is that there is an approximate equilibrium between floristic temperature and observed temperature during the period used for model calibration (our Baseline period). Since we have a dataset covering multiple decades and across different geographical areas, we could confirm that species assemblages in the baseline datasets were in a relatively stable equilibrium before the recent global warming (**Figure S13**). It is also reassuring that our analyses reveal both floristic temperature anomaly and thermal lag responses in the period prior to our Baseline period (Historic period, 1905–1949), and that we find a negative lag when temperatures were particularly colder (during the 1920s) and a positive lag when temperatures were warmer (during the 1930–40s) (Figure 2). Nevertheless, these deviations are still substantially smaller than those observed during the Contemporary time period. It is also important to consider that as long as we account for observed temperature change, it is equally valid to understand the described correlations with thermal lag as the correlation with the floristic temperature anomaly.

Assemblages are composed of individual species that respond to changes in their environment depending on their niche requirements. Hence, species do not necessarily respond synchronously in space and time to warming. However, our results suggest a generalized species response to temperature-change velocity. Including abundance data and functional groups might help to give a more detailed picture of the shifting dominance of functional groups and species within assemblages and subsequently to understand the consequences of assemblage reorganizations in response to global warming (Kullman, 2004; Rumpf et al., 2019). Finally, we highlight that, although we focus in our study on temperature change, combined effects with other climatic factors, such as precipitation (Feeley et al., 2020) or vegetation structure (Richard et al., 2021) and non-climatic factors, such as land-use change or populations dynamics (Bertrand, 2019), are needed in future studies to achieve a holistic perspective of drivers of the thermal lags in plant assemblages.

5 | CONCLUSIONS

Lagged responses in plant assemblages have a profound impact on vegetation functioning and ecosystem dynamics. Overall, we find an increasing floristic temperature anomaly (i.e. thermophilization) of the Norwegian plant assemblages during the last century, but also an increasing thermal lag as global warming outpaces species response. Additionally, our results suggest that thermal lags are associated with different dimensions of temperature-change velocity on a broad landscape scale. More specifically, our study shows that the magnitude of thermal lags depends on the additive effect of temperature-change velocity, distance to analogous thermal conditions, baseline temperatures, and the length of time over which the temperature change occurs. These factors might limit species' range shifts to keep track of their thermal niche under changing climate conditions and can result in increasing lags due to migration distance and low thermophilization. However, it remains uncertain how large the thermal lag can increase over time before critical tipping points are reached that threaten vegetation and ecosystem functioning. For instance, the observed thermal lag may reflect that the species live in suboptimal thermal conditions, potentially making them vulnerable to other factors, such as habitat fragmentation and destruction, or which could hinder their mobility in the landscape. Our study exemplifies that thermal lags are the result of very complex spatio-temporal processes. These responses need to be considered jointly to be able to obtain solid risk assessments of biodiversity responses to global warming and

to be able to predict the magnitude of critical consequences for ecosystems and human well-being.

REFERENCES

Alexander, J. M., Chalmandrier, L., Lenoir, J., Burgess, T. I., Essl, F., Haider, S., … Pellissier, L. (2018). Lags in the response of mountain plant communities to climate change. *Global Change Biology*, *24*(2), 563–579. https://doi.org/10.1111/gcb.13976

Amatulli, G., Domisch, S., Tuanmu, M., Parmentier, B., Ranipeta, A., Malczyk, J., & Jetz, W. (2018). Data Descriptor : A suite of global , cross-scale topographic variables for environmental and biodiversity modeling. *Sci Data*, *5*(180040), 1–15. https://doi.org/https://doi.org/10.1038/sdata.2018.40

Andrews, D. W. K. (1993). Tests for Parameter Instability and Structural Change With Unknown Change Point. *Econometrica*, *61*(4), 821–856. https://doi.org/10.2307/2951764

Beale, C. M., Lennon, J. J., Yearsley, J. M., Brewer, M. J., & Elston, D. A. (2010). Regression analysis of spatial data. *Ecology Letters*, *13*(2), 246–264. https://doi.org/10.1111/j.1461-0248.2009.01422.x

Bertrand, R. (2019). Unequal contributions of species' persistence and migration on plant communities' response to climate warming throughout forests. *Ecography*, *42*(1), 211–213. https://doi.org/10.1111/ecog.03591

Bertrand, R., Lenoir, J., Piedallu, C., Dillon, G. R., De Ruffray, P., Vidal, C., … Gégout, J. C. (2011). Changes in plant community composition lag behind climate warming in lowland forests. *Nature*, *479*(7374), 517–520. https://doi.org/10.1038/nature10548

Bertrand, R., Riofrío-Dillon, G., Lenoir, J., Drapier, J., De Ruffray, P., Gégout, J. C., & Loreau, M. (2016). Ecological constraints increase the climatic debt in forests. *Nature Communications*, *7*. https://doi.org/10.1038/ncomms12643

Bhatta, K. P., Birks, H. J. B., Grytnes, J.-A., & Vetaas, O. R. (2019). Weighted average regression and environmental calibration as a tool for quantifying climate-driven changes in vegetation. *Journal of Plant Ecology*, *12*(4), 787–789. https://doi.org/10.1093/jpe/rtz015

Bhatta, K. P., Grytnes, J. A., & Vetaas, O. R. (2018). Downhill shift of alpine plant assemblages under contemporary climate and land-use changes. *Ecosphere*, *9*(1). https://doi.org/10.1002/ecs2.2084

Birks, H. J. B., & Simpson, G. L. (2013). Diatoms and pH reconstruction (1990) revisited. *Journal of Paleolimnology*, *49*(3), 363–371. https://doi.org/10.1007/s10933-013-9697-7

Blonder, B., Nogués-Bravo, D., Borregaard, M. K., Donoghue, J. C., Jørgensen, P. M., Kraft, N. J. B., … Enquist, B. J. (2015). Linking environmental filtering and disequilibrium to biogeography with a community climate framework. *Ecology*, *96*(4), 972–985. https://doi.org/10.1890/14-0589.1

Chen, I.-C., Hill, J. K., Ohlemüller, R., Roy, D. B., & Thomas, C. D. (2011). Rapid range shifts of species associated with high levels of climate warming. *Science*, *333*(6045), 1024–1026. https://doi.org/10.1126/science.1206432

Chevalier, M., Davis, B. A. S., Heiri, O., Seppä, H., Chase, B. M., Gajewski, K., … Kupriyanov, D. (2020). Pollen-based climate reconstruction techniques for late Quaternary studies. *Earth-Science Reviews*, *210*(May), 103384. https://doi.org/10.1016/j.earscirev.2020.103384

Copernicus. (2016). European Digital Elevation Model EU-DEM v1.1. Retrieved from https://land.copernicus.eu/imagery-in-situ/eu-dem/eu-dem-v1.1?tab=metadata

De Frenne, P., Rodríguez-Sánchez, F., Coomes, D. A., Baeten, L., Verstraeten, G., Vellen, M., … Verheyen, K. (2013). Microclimate moderates plant responses to macroclimate warming. *Proceedings of the National Academy of Sciences of the United States of America*, *110*(46), 18561–18565. https://doi.org/10.1073/pnas.1311190110

De Frenne, P., Zellweger, F., Rodríguez-Sánchez, F., Scheffers, B. R., Hylander, K., Luoto, M., … Lenoir, J. (2019). Global buffering of temperatures under forest canopies. *Nature Ecology and Evolution*, *3*(5), 744–749. https://doi.org/10.1038/s41559-019-0842-1

Dorman, M., Rush, J., Hough, I., Russel, D., & Karney, C. F. . (2020). *nngeo: k-Nearest Neighbor Join for Spatial Data*. Retrieved from https://michaeldorman.github.io/nngeo/

Feeley, K. J., Bravo-Avila, C., Fadrique, B., Perez, T. M., & Zuleta, D. (2020). Climate-driven changes in the composition of New World plant communities. *Nature Climate Change*, *10*(10), 965–970. https://doi.org/10.1038/s41558-020-0873-2

Freeman, B., Song, Y., Feeley, K. J., & Zhu, K. (2021). Montane species track rising temperatures better in the tropics than in the temperate zone. *Ecology Letters*, *24*, 1697–1708. https://doi.org/10.1111/ele.13762

Garcia, R. A., Cabeza, M., Rahbek, C., & Araújo, M. B. (2014). Multiple Dimensions of Climate Change and Their Implications for Biodiversity. *Science*, *344*(6183). https://doi.org/10.1126/science.1247579

Gottfried, M., Pauli, H., Futschik, A., Akhalkatsi, M., Barančok, P., Benito Alonso, J. L., … Grabherr, G. (2012). Continent-wide response of mountain vegetation to climate change. *Nature Climate Change*, *2*(2), 111–115. https://doi.org/10.1038/nclimate1329

Graae, B. J., Vandvik, V., Armbruster, W. S., Eiserhardt, W. L., Svenning, J. C., Hylander, K., … Lenoir, J. (2018). Stay or go – how topographic complexity influences alpine plant population and community responses to climate change. *Perspectives in Plant Ecology, Evolution and Systematics*, *30*, 41–50. https://doi.org/10.1016/j.ppees.2017.09.008

Grytnes, J. A., Kapfer, J., Jurasinski, G., Birks, H. J. B. H., Henriksen, H., Klanderud, K., … Birks, H. J. B. H. (2014). Identifying the driving factors behind observed elevational range shifts on European mountains. *Global Ecology and Biogeography*, *23*(8), 876–884. https://doi.org/10.1111/geb.12170

Hijmans, Robert J. ; van Etten, J. (2012). *raster: Geographic analysis and modeling with raster data. R package version 2.5-8.*

Hutchinson, G. E. (1957). Concluding remarks. *Population Studies: Animal Ecology and Demography. Cold Spring Harbor Symposium on Quantitative Biology*, *22*, 415–457. https://doi.org/10.1007/BF02464429

Ives, A., & Li, D. (2018). rr2: An R package to calculate R^2s for regression models. *Journal of Open Source Software*, *3*, 1028. https://doi.org/10.21105/joss.01028

Jackson, S. T., & Sax, D. F. (2010). Balancing biodiversity in a changing environment: extinction debt, immigration credit and species turnover. *Trends in Ecology and Evolution*. https://doi.org/10.1016/j.tree.2009.10.001

Jump, A. S., Mátyás, C., & Peñuelas, J. (2009). The altitude-for-latitude disparity in the range retractions of woody species. *Trends in Ecology and Evolution*, *24*(12), 694–701.

https://doi.org/10.1016/j.tree.2009.06.007

Karger, D. N., Conrad, O., Böhner, J., Kawohl, T., Kreft, H., Soria-Auza, R. W., … Kessler, M. (2017). Climatologies at high resolution for the earth's land surface areas. *Scientific Data*, *4*, 1–20. https://doi.org/10.1038/sdata.2017.122

Karger, D. N., & Zimmermann, N. E. (2018). *CHELSAcruts - High resolution temperature and precipitation timeseries for the 20th century and beyond*. https://doi.org/10.16904/envidat.159

Kassambara, A. (2020). *ggpubr: "ggplot2" Based Publication Ready Plots. R package version 0.4.0*. Retrieved from https://cran.r-project.org/package=ggpubr

Kullman, L. (2004). Long-term geobotanical observations of climate change impacts in the Scandes of West-Central Sweden. *Nordic Journal of Botany*, *24*(4), 445–467. https://doi.org/10.1111/j.1756-1051.2004.tb02209.x

Lenoir, J., Bertrand, R., Comte, L., Bourgeaud, L., Hattab, T., Murienne, J., & Grenouillet, G. (2020). Species better track climate warming in the oceans than on land. *Nature Ecology and Evolution*. https://doi.org/10.1038/s41559-020-1198-2

Lenoir, J., Graae, B. J., Aarrestad, P. A., Alsos, I. G., Armbruster, W. S., Austrheim, G., … Svenning, J. C. (2013). Local temperatures inferred from plant communities suggest strong spatial buffering of climate warming across Northern Europe. *Global Change Biology*, *19*(5), 1470–1481. https://doi.org/10.1111/gcb.12129

Lenoir, J., & Svenning, J. C. (2015). Climate-related range shifts - a global multidimensional synthesis and new research directions. *Ecography*, *38*(1), 15–28. https://doi.org/10.1111/ecog.00967

Liu, M., Prentice, I. C., Ter Braak, C. J. F., & Harrison, S. P. (2020). An improved statistical approach for reconstructing past climates from biotic assemblages: Improved palaeoclimate reconstruction. *Proceedings of the Royal Society A: Mathematical, Physical and Engineering Sciences*, *476*(2243). https://doi.org/10.1098/rspa.2020.0346

Loarie, S. R., Duffy, P. B., Hamilton, H., Asner, G. P., Field, C. B., & Ackerly, D. D. (2009). The velocity of climate change. *Nature*, *462*(7276), 1052–1055. https://doi.org/10.1038/nature08649

NIBIO. (2021). Corine Landcover 2000, 2006 and 2012 (CLC) - Arealdekke. Retrieved from

Geonorge website: https://kartkatalog.geonorge.no/

Norwegian University of Life Sciences (NMBU). (2019). Vascular Herbarium, NMBU. Version 1.180. Occurrence dataset. https://doi.org/10.15468/mbhmmt

Norwegian University of Science and Technology. (2021). Vascular plant field notes, NTNU University Museum. Version 1.101. Sampling event dataset. https://doi.org/10.15468/kkb2x0

O'Sullivan, K. S. W., Ruiz-Benito, P., Chen, J. C., & Jump, A. S. (2021). Onward but not always upward: individualistic elevational shifts of tree species in subtropical montane forests. *Ecography*, *44*(1), 112–123. https://doi.org/10.1111/ecog.05334

Oksanen, J., Blanchet, F. G., Kindt, R., Legendre, P., Minchin, P. R., O'hara, R. B., … Wagner, H. (2013). Package 'vegan.' *Community Ecology Package,* Vol. 2. Retrieved from https://github.com/vegandevs/vegan

Pebesma, E. (2018). Simple Features for R: Standardized Support for Spatial Vector Data. *R Journal*, *10*, 439–446. https://doi.org/10.32614/RJ-2018-009

Pinheiro, J., Bates, D., DebRoy, S., & Sarkar, D. (2020). *R Core Team (2020) nlme: Linear and Nonlinear Mixed Effects Models. R package version 3.1–149*. Retrieved from https://cran.r-project.org/package=nlme.

R Core Team. (2021). *R: A Language and Environment for Statistical Computing*. Retrieved from https://www.r-project.org/

Richard, B., Dupouey, L., Corcket, E., Alard, D., Archaux, F., Aubert, M., … Lenoir, J. (2021). The climatic debt is growing in the understorey of temperate forests : Stand characteristics matter. *Global Ecology and Biogeography*, (March), 1474–1487. https://doi.org/10.1111/geb.13312

Riley, S. J., DeGloria, S. D., & Elliot, R. (1999). Index that quantifies topographic heterogeneity. *Intermountain Journal of Sciences*, *5*(1–4), 23–27.

Riofrío-Dillon, G., Bertrand, R., & Gégout, J.-C. (2012). Toward a recovery time: forest herbs insight related to anthropogenic acidificatio. *Global Change Biology*, *18*, 3383–3394. https://doi.org/10.1111/gcb.12002

Rumpf, S. B., Hülber, K., Klonner, G., Moser, D., Schütz, M., Wessely, J., … Dullinger, S.

(2018). Range dynamics of mountain plants decrease with elevation. *Proceedings of the National Academy of Sciences of the United States of America*, *115*(8), 1848–1853. https://doi.org/10.1073/pnas.1713936115

Rumpf, S. B., Hülber, K., Wessely, J., Willner, W., Moser, D., Gattringer, A., … Dullinger, S. (2019). Extinction debts and colonization credits of non-forest plants in the European Alps. *Nature Communications*, *10*(1), 1–9. https://doi.org/10.1038/s41467-019-12343-x

Salonen, J. S., Ilvonen, L., Seppä, H., Holmström, L., Telford, R. J., Gaidamavičius, A., … Subetto, D. (2011). Comparing different calibration methods (WA/WA-PLS regression and Bayesian modelling) and different-sized calibration sets in pollen-based quantitative climate reconstruction. *The Holocene*, *22*(4), 413–424. https://doi.org/10.1177/0959683611425548

Steinbauer, M. J., Grytnes, J.-A., Jurasinski, G., Kulonen, A., Lenoir, J., Pauli, H., … Wipf, S. (2018). Accelerated increase in plant species richness on mountain summits is linked to warming. *Nature*, *556*(7700), 231–234. https://doi.org/10.1038/s41586-018-0005-6

Svenning, J. C., & Sandel, B. (2013). Disequilibrium vegetation dynamics under future climate change. *American Journal of Botany*, *100*(7), 1266–1286. https://doi.org/10.3732/ajb.1200469

ter Braak, C. J. F., & Juggins, S. (1993). Weighted averaging partial least squares regression (WA-PLS): an improved method for reconstructing environmental variables from species assemblages. *Hydrobiologia*, *269–270*(1), 485–502. https://doi.org/10.1007/BF00028046

The Global Biodiversity Information Facility, G. (2020). GBIF.org. Retrieved January 20, 2020, from Species matching website: https://www.gbif.org/tools/species-lookup

University of Agder. (2021). Vascular plant herbarium (KMN) UiA. Version 1.1804. Occurrence dataset. https://doi.org/10.15468/2g6i0v

University of Oslo. (2019a). Vascular Plants, Field notes, Oslo (O). Version 1.186. Occurrence dataset. https://doi.org/10.15468/w8gru5

University of Oslo. (2019b). Vascular Plants, Observations, Oslo (O). Version 1.181. Occurrence dataset. https://doi.org/10.15468/tvnjk7

Wickham, H., Averick, M., Bryan, J., Chang, W., McGowan, L., François, R., … Yutani, H. (2019). Welcome to the Tidyverse. *Journal of Open Source Software*, *4*, 1686. https://doi.org/10.21105/joss.01686

Zeileis, A., Leisch, F., Homik, K., & Kleiber, C. (2002). strucchange: An R Package for Testing for Structural Change. *Journal of Statistical Software*, *7*(2), 1–38.

Zellweger, F., Frenne, P. De, Lenoir, J., Vangansbeke, P., Verheyen, K., Baeten, L., … Coomes, D. (2020). Forest microclimate dynamics drive plant responses to warming. *Science*, *775*(June), 772–775. https://doi.org/10.1126/science.aba6880

TABLES

Table 1. Generalized least square models of the variation of plant assemblages' thermal lags related to time (year) for the whole period (1905–2007) and the contemporary period (1980–2007) using the temporal-spatial corrected subset.

Period		Year	Obs	R^2
1905-2007	*Estimates*	4.9×10^{-3}	3045	0.079
	Std error	9×10^{-4}		
	P-value	**<0.001**		
1980-2007	*Estimates*	4.9×10^{-2}	850	0.093
	Std error	5.5×10^{-3}		
	P-value	**<0.001**		

Std error = standard error; Obs =number of assemblages included in the models.

Table 2. Generalized least square models of the variation of plant assemblages' thermal lags related to temperature-change velocity, baseline temperature conditions, topographic heterogeneity, and forest: time, distance to past analogous thermal conditions, rate of temperature change, magnitude of temperature change and baseline temperature, elevation, terrain ruggedness, geomorphological landform diversity, and forest cover.

	Model		Year	Dist to analog past thermal conditions (log)	Rate of temp change	Magnitude temp change	Baseline temp	R^2	AIC	Obs
Temperature-change velocity and Baseline temperature conditions	*1*	*Estimates*	0.038					0.041	19244	6208
		Std error	0.002							
		P-value	**<0.001**							
	2	*Estimates*	0.038	0.142				0.054	20691	
		Std error	0.002	0.014						
		P-value	**<0.001**	**<0.001**						
	3	*Estimates*	0.024		2.13			0.055	20683	
		Std error	0.002		0.204					
		P-value	**<0.001**		**<0.001**					
	4	*Estimates*				0.701		0.076	20535	
		Std error				0.030				
		P-value				**<0.001**				
	5	*Estimates*	0.038				0.022	0.041	20776	
		Std error	0.002				0.006			
		P-value	**<0.001**				**<0.001**			
	6	*Estimates*	0.02	0.011	1.848		-0.011	0.126	19134	
		Std error	0.003	0.017	0.230		0.015			
		P-value	**<0.001**	**<0.001**	**<0.001**		0.467			
	7	*Estimates*		0.079		0.646	0.013	0.082	20496	
		Std error		0.015		0.032	0.006			
		P-value		**<0.001**		**<0.001**	**0.041**			

	Model		Year	Elevation	Shannon Landforms	Ruggedness	Forest cover	R^2	AIC
Topographic heterogeneity and forest cover	*8*	*Estimates*	0.038	0				0.040	19246
		Std error	4.580	0					
		P-value	**<0.001**	0.656					
	9	*Estimates*	0.038		0.006			0.040	19246
		Std error	0.002		0.033				
		P-value	**<0.001**		0.85				
	10	*Estimates*	0.038			-0.006		0.041	19244
		Std error	0.002			0.002			
		P-value	**<0.001**			**<0.001**			
	11	*Estimates*	0.04				-0.11	0.042	20775

	Std error	0.002				0.029		
	P-value	**<0.001**				**<0.001**		
	Estimates	0.04	0	0.00	-0.001	-0.01		
12	*Std error*	0.002	0	0.034	0.004	0.031	0.042	19249
	P-value	**<0.001**	0.511	0.896	0.100	0.728		

Std error = standard error; Dist = distance; temp = temperature; Obs = number of assemblages included in the models.

Table 3. Generalized least square models of the variation of plant assemblages' thermal lags testing the relation with several potential determinants related to time, temperature-change velocity, baseline temperature conditions, topographic heterogeneity, and forest cover. The correlation values among all the determinants included in each of the full models do not exceed a Spearman's r coefficient of 0.6.

	Model 13			*Model 14*		
Determinant	*Estimates*	*Std error*	*P-value*	*Estimates*	*Std error*	*P-value*
Year	0.02	0.003	**<0.001**			
Rate of temp change	1.87	0.230	**<0.001**			
Dist analog past thermal conditions (log)	0.11	0.017	**<0.001**	0.04	0.018	**0.020**
Baseline temp	-0.01	0.015	0.407	0.01	0.015	0.641
Ruggedness	-0.01	0.004	0.115	-0.01	0.003	0.065
Shannon landforms	-0.01	0.033	0.772	-0.00	0.033	0.828
Forest cover	0.01	0.032	0.714	-0.00	0.032	0.962
Magnitude temp change				0.70	0.037	**<0.001**
R^2		0.126			0.145	
AIC		19138			19020	
Obs			6208			

Std error = standard error; temp = temperature; Dist = Distance (to); Obs = number of assemblages included in the models.

FIGURES

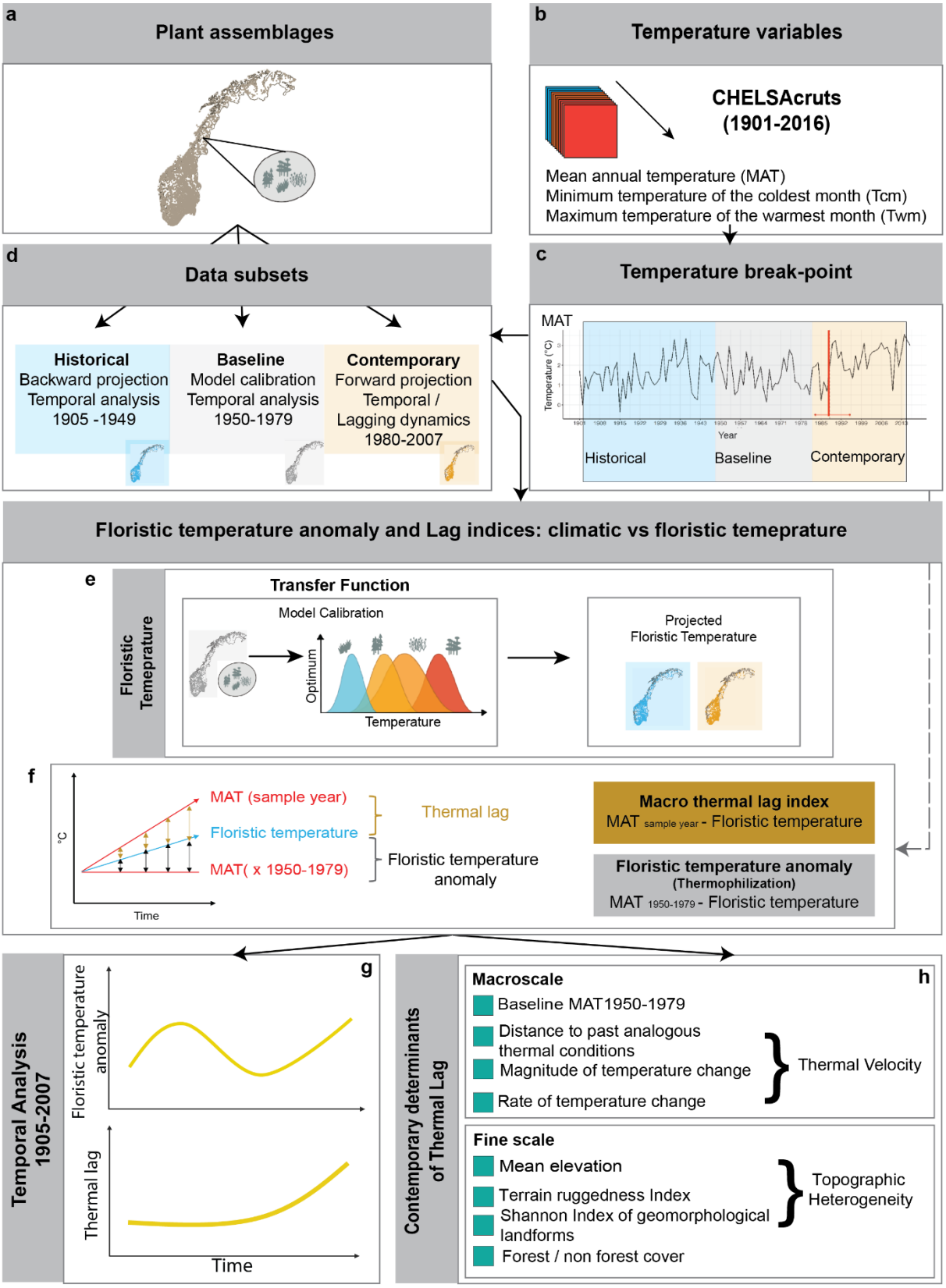

Figure 1. | Workflow of our study from top to bottom.

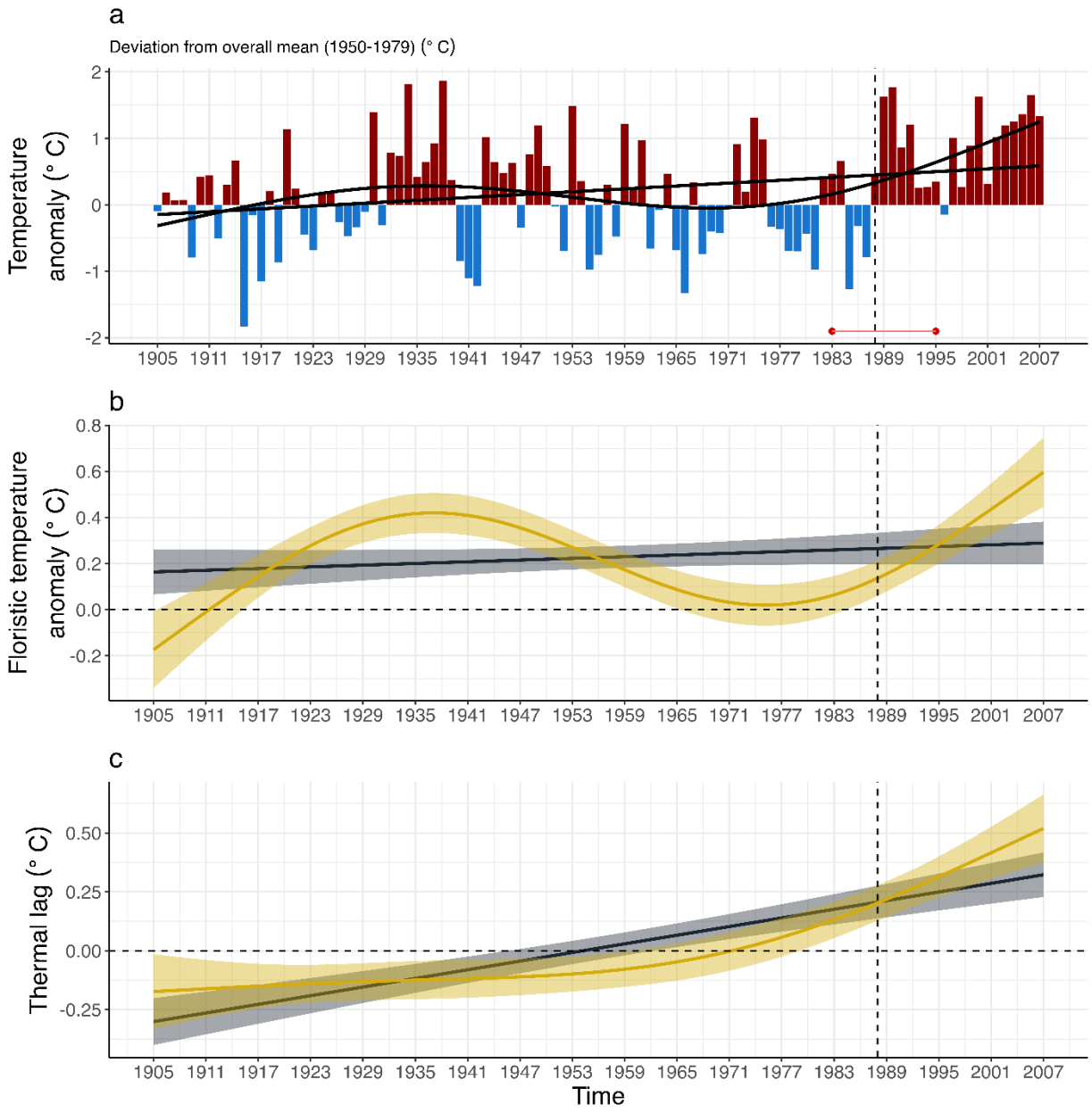

Figure 2 | a) Temperature anomaly for Norway since 1905. Deviation from overall mean of 1950–1979 mean. Black lines are linear and generalized additive model (k=4) regressions, horizontal bright red line shows breaking point confidence interval (95% CI from 1983 to 1995). b) Temporal trends of floristic temperature anomaly based on the bias corrected dataset. c) Thermal lag index of the bias corrected dataset. For b) and c) the black line is a linear regression of the temporal generalized linear model; yellow line is a generalized additive model. Vertical dashed lines mark the start of the current global warming period as defined by the break-point analyses (1988).

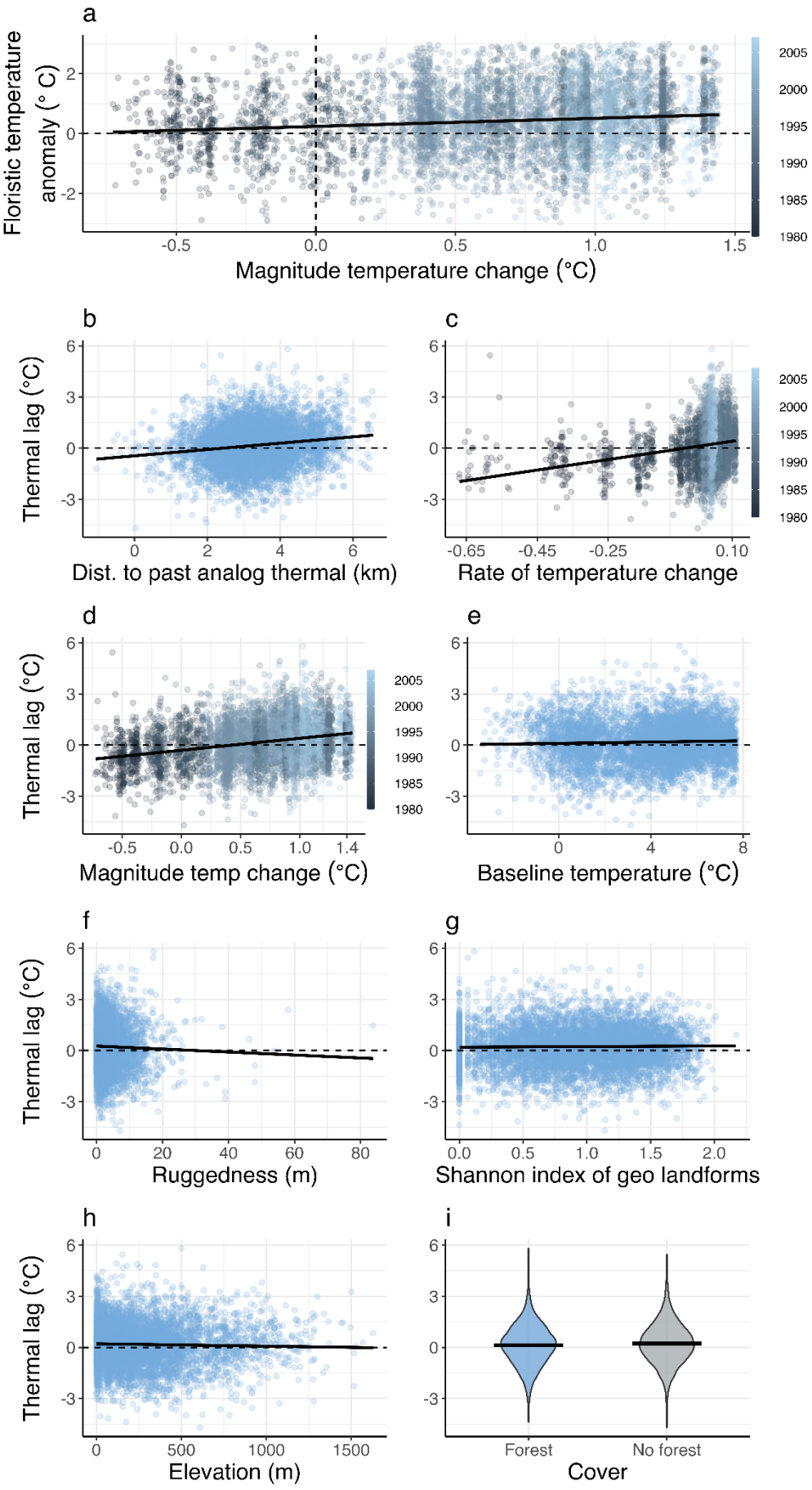
a
Floristic temperature anomaly (° C)
Magnitude temperature change (°C)
2005
2000
1995
1990
1985
1980
b
Thermal lag (°C)
Dist. to past analog thermal (km)
c
Rate of temperature change
d
Magnitude temp change (°C)
e
Baseline temperature (°C)
f
Ruggedness (m)
g
Shannon index of geo landforms
h
Elevation (m)
i
Forest
No forest
Cover

858

Figure 3 | a) Relationship between magnitude of temperature change and floristic temperature anomaly. Relationships between the thermal lag index and the following predictor variables: b) Distance to past analogous climatic conditions (log-transformed), c) Rate of temperature change, d) Magnitude of temperature change, e) Baseline temperature, f) Terrain ruggedness index, g) Shannon index of geomorphological landforms, h) Elevation, and i) Forest cover. Lines represent the fit of the univariate generalized least square (GLS) models (Table 3 and Table 4). Each point represents a plant assemblage in the Contemporary dataset (1980–2007). The color bars in a, c, and d reflect the year of assemblage sampling.

DATA ACCESSIBILITY STATEMENT

The data that support the findings of this study are openly available in GBIF at the following DOIs: University of Agder (2022). Vascular plant herbarium (KMN) UiA https://doi.org/10.15468/2g6i0v, University of Oslo https://doi.org/10.15468/w8gru5, https://doi.org/10.15468/tvnjk7, Norwegian University of Science and Technology https://doi.org/10.15468/kkb2x0, Norwegian University of Life Sciences (NMBU) https://doi.org/10.15468/mbhmmt. The climate data used are available from https://chelsa-climate.org/chelsacruts/. R scripts used to produce the main results can be found on Zenodo (https://doi.org/10.5281/zenodo.6998063). The species list is provided in the Supporting Information (**Table S1**).

TITLES OF SUPPLEMENTARY FILES

Figure S1: Frequency distribution of plant assemblages

Figure S2: Non-metric multidimensional scaling (NMDS) ordination of plant assemblages

Figure S3: Breaking point statistics

Figure S4: Location of the plant assemblages across Norway

Figure S5: Transfer function – Floristic temperature

Figure S6: Thermal lag of the complete dataset using different baseline periods

Figure S7: Subdivision zones of Norway to perform stratified random sampling

Figure S8: Longitudinal and latitudinal trends of the species assemblages

Figure S9: Thermal lag trends from the Complete dataset and Bias-corrected dataset

Figure S10: Relationship between elevation and terrain ruggedness index

Figure S11: Variograms of the models residuals